Silencing of p29 Affects DNA Damage Responses with UV Irradiation

Po-Chen Chu,[1] Yuh-Cheng Yang,[2,3,5] Yen-Ta Lu,[2,4,5] Hsiang-Ting Chen,[2] Lung-Chih Yu,[1] and Mau-Sun Chang[2,6]

[1]Institute of Biochemical Sciences, National Taiwan University; [2]Department of Medical Research, Mackay Memorial Hospital; Departments of [3]Obstetrics and Gynecology and [4]Respiratory Care, Taipei Medical University; [5]Mackay Medicine, Nursing and Management College; and [6]National Taipei University of Technology, Taipei, Taiwan

Abstract

Human p29 is a newly identified nuclear protein whose function is largely undetermined. We found that p29 associated with chromatin, interacted with MCM3, and localized with proliferating cell nuclear antigen foci in the S phase. Silencing of p29 using small interfering RNA duplexes reduced DNA synthesis and increased the expression of p107, a member of the RB family, and of cyclin-dependent kinase inhibitor p21, accompanied with a decreased expression of DNA polymerase α. Lethal events consisting of premature chromatin condensation with a reduced Chk1 phosphorylation were observed in p29-depleted cells in response to UV irradiation. Intriguingly, the phosphorylation of ataxia telangectasia-mutated kinases at S1981 was suppressed in p29-depleted HeLa cells with UV irradiation, but not in hydroxyurea- and ionizing radiation-treated cells. Taken together, these results reveal a novel function of p29 in the regulation of DNA replication checkpoint responses. (Cancer Res 2006; 66(17): 8484-91)

Introduction

During the eukaryotic cell cycle, events in the G_1 and S phases are exquisitely controlled by a multitude of regulators to ensure high fidelity during each round of DNA replication. These regulators include complexes of cyclin-dependent kinases (Cdk4/6) and cyclin D (1–3). Cdk/cyclin D complex activity is responsible for the phosphorylation and inactivation of the retinoblastoma susceptibility gene product, RB. Upon phosphorylation of RB by Cdk4/6-cyclin D, dissociation of RB from E2F results in E2F-mediated transcriptional activation of critical S phase effectors, including cyclin E, cyclin A, Orc1, Cdc6, and DNA polymerase α (4). Pocket proteins, composed of RB, p107, and p130, interact with E2Fs to function in cell cycle progression. RB preferentially binds to activator E2F1, E2F2, and E2F3. In contrast, p107 and p130 bind repressor E2F4 and E2F5 to selectively inhibit distinct sets of genes (5, 6).

An effective response to damaged or abnormally replicated DNA in the mammalian cell cycle is propagated by the DNA damage checkpoint pathway. The signal transducing kinases, ATM (ataxia telangectasia-mutated), ATR (ataxia telangectasia and Rad3-related), Chk1, and Chk2, phosphorylate downstream checkpoint effector proteins, such as Cdc25, p53, and E2F, to regulate cellular responses and ensure error-free DNA replication (6–10). It is believed that ATM responds primarily to double-strand breaks through the Mre11-Rad50-Nbs1 complex (11–13). The DNA damage in the S phase in response to UV irradiation or replication stress leads to the production of RPA-ssDNA complex, which facilitates the binding of ATR and ATR-mediated phosphorylation of Chk1. The activated Chk1 kinase phosphorylates downstream targets causing cell cycle arrest or apoptosis (14–16).

p29 was initially identified as interacting with GCIP in yeast two-hybrid screening (17). GCIP associates with cyclin D and phosphorylation of the RB protein is inhibited in the presence of GCIP. E2F1 transcriptional activity is suppressed in cells transfected with GCIP (18). Nevertheless, it is unclear whether p29 can affect the stability of cyclin D or E2F-mediated transcription. To further decipher the function of the p29 protein, we investigated the consequences of p29 depletion in response to genotoxic stress.

Materials and Methods

Antibodies. Purified 6×His-tagged p29 were prepared to produce monoclonal antibodies. Antibodies against β-tubulin, cyclin A, p21, p107, p130, Chk1, Chk2, and ATR were purchased from Santa Cruz Biotech (Santa Cruz, CA). Anti-RB monoclonal antibody was from BD PharMingen (San Diego, CA). Anti-p53, bromodeoxyuridine (BrdUrd), RPA1, and RPA2 monoclonal antibodies were from Neomarkers (Fremont, CA). Rabbit anti-ATM and anti-pATM S1981 antibodies were from Novus Biologicals (Littleton, CO) and Rockland Immunochemicals (Gilbertsville, PA). Rabbit anti-pChk1 S317, S345, anti-pChk2 T68, and anti-pRad17 S645 antibodies were from Cell Signaling (Beverly, MA).

Whole cell extracts, nuclear extracts, and chromatin isolation. Cell extracts were prepared as previously described (19). Briefly, whole cell extracts were lysed with radioimmunoprecipitation assay buffer. To prepare cytosolic and nuclear extracts, the cells were lysed by Dounce homogenization in hypotonic buffer [20 mmol/L Hepes-KOH (pH 8.0), 5 mmol/L KCl, 1.5 mmol/L $MgCl_2$, 5 mmol/L sodium butyrate, 0.1 mmol/L DTT, and protease inhibitors]. The cytosolic extracts were clarified by high-speed centrifugation (15 minutes, 13,500 rpm, 4°C). Nuclei were collected by centrifugation (5 minutes, 2,000 rpm, 4°C) and resuspended in nuclear extraction buffer [15 mmol/L Tris-HCl (pH 7.5), 1 mmol/L EDTA, 0.4 mol/L NaCl, 10% sucrose, 1 mmol/L DTT, and protease inhibitors]. Insoluble proteins were removed from the nuclear extracts by high-speed centrifugation (20 minutes, 13,500 rpm, 4°C). To isolate chromatin-associated proteins, nuclei from 1×10^8 cells were resuspended in buffer A [10 mmol/L HEPES (pH 7.9), 10 mmol/L KCl, 1.5 mmol/L $MgCl_2$, 0.34 mol/L sucrose, 10% glycerol, 1 mmol/L DTT, 0.1% Triton X-100, and protease inhibitors] plus 0.2 units of micrococcal nuclease (Sigma-Aldrich, St. Louis, MO). After incubation at 37°C for 1 minute, nuclei were collected and lysed in 1 mL of buffer B (3 mmol/L EDTA, 0.2 mmol/L EGTA, 1 mmol/L DTT, protease inhibitors). Insoluble chromatin was collected by centrifugation (5 minutes, 2,500 rpm, 4°C) and resuspended in 0.5 mL Laemmli buffer, sonicated for

Note: P-C. Chu and Y-C. Yang contributed equally to this article.

Requests for reprints: Mau-Sun Chang, Department of Medical Research, Mackay Memorial Hospital, 45 Minshen Road, Tamshui, Taipei, Taiwan. Phone: 886-2-2809-4661, ext. 3081; Fax: 886-2-2808-5952; E-mail: mschang@ms1.mmh.org.tw.

doi:10.1158/0008-5472.CAN-05-3229

5 minutes, and spun down to collect chromatin-associated proteins. Chromatin immunoprecipitation was done as described previously (20).

Immunofluorescence. HeLa cells were preextracted with cytoskeleton extraction buffer [10 mmol/L Pipes-KOH (pH 7.0), 150 mmol/L NaCl, 300 mmol/L sucrose, 3 mmol/L $MgCl_2$, 0.5% Triton X-100, 0.5 mmol/L phenylmethylsulfonyl fluoride, and protease inhibitors] and then fixed in cold methanol (−20°C). To visualize the incorporation of BrdUrd, cells were pulse-labeled with 10 μmol/L of BrdUrd for 30 minutes and then chased in BrdUrd-free medium for 30 minutes. Cells were fixed in methanol and denatured with 2 mol/L HCl for 30 minutes. Immunostained images were visualized and recorded using a Leica confocal laser scanning microscope (Leica, Germany).

Small interfering RNA. Two small interfering RNA (siRNA) duplexes were designed corresponding to the coding regions 92 to 112 and 440 to 460 nucleotides relative to the start codon of p29 (GenBank accession no., AF273089). For the control experiment, firefly (*Photinus pyralis*) luciferase (accession no., X65324) at positions 153 to 173 was used. All of the siRNA duplexes were synthesized by Dharmacon Research, Inc. (Lafayette, CO).

UV irradiation. UV light was delivered by the UV Stratalinker 2400 (Stratagene, La Jolla, CA).

Detection of apoptotic cells. HeLa cells were transfected with siRNA duplexes. Apoptotic cells were labeled with FITC-conjugated Annexin V (Sigma-Aldrich) and propidium iodide for 15 minutes in the dark and analyzed by FACSCalibur (Becton Dickinson, Mountain View, CA).

Mitotic spreads. Mitotic spreads were carried out as described previously (21, 22). Briefly, siRNA-transfected cells were UV-irradiated and incubated with nocodazole (0.1 mg/mL) for 16 hours. Cells were incubated with 75 mmol/L of KCl for 30 minutes at room temperature and resuspended in three changes of 300 μL of freshly prepared Carnoy's fixative (three parts methanol, one part glacial acetic acid), each for 10 minutes at room temperature. Cells were resuspended in 100 μL of Carnoy's fixative, dropped onto a glass slide, and stained with 4′,6-diamidino-2-phenylindole. A coverslip was placed onto the slide and the edges were sealed with nail polish.

Results

p29 associates with chromatin. The specificity of anti-p29 monoclonal antibody was determined by Western blot analysis using HeLa cell extracts (Fig. 1*A*). Subcellular fractionation showed that p29 was not present in the cytosolic fraction (Fig. 1*B*, cytosolic extracts), and there was only a small amount in the nuclear soluble fraction (Fig. 1*B*, nuclear extracts). In contrast, p29 was abundantly associated with chromatin (Fig. 1*B*, chromatin-enriched fraction). To detect chromatin-associated p29 by immunofluorescence, HeLa cells were preextracted with 0.5% Triton X-100. p29 bound to chromatin after Triton X-100 extraction and was released from the nucleus by DNase I treatment (Fig. 1*C*). The control experiment showed that MCM3 associated with chromatin and was retained in the nucleolus after DNase I treatment (Fig. 1*C*).

During the immunofluorescent studies on the localization of p29, some cells showed fewer nuclear signals. We speculated that p29 might be distributed in a cell cycle–dependent manner. To verify this hypothesis, HeLa cells were synchronized at the G_1-S

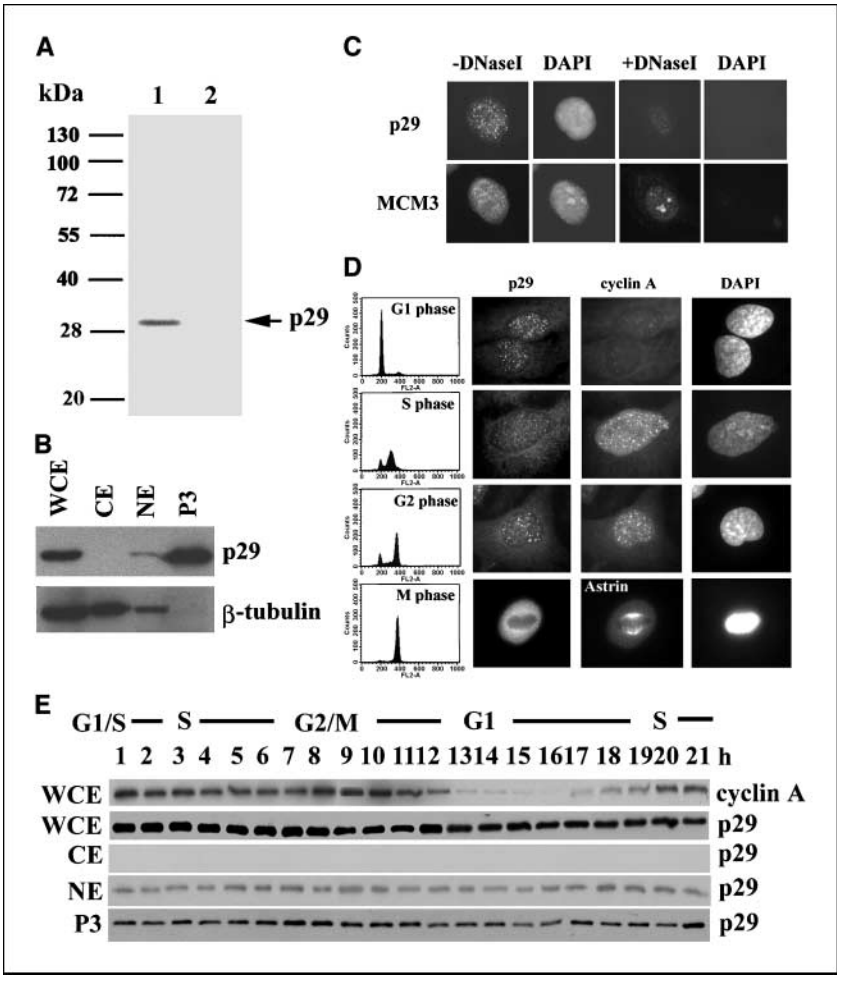

Figure 1. Association of p29 with chromatin. *A,* whole cell extracts of HeLa cells were blotted with anti-p29 monoclonal antibody (*lane 1*). Immuno-neutralization test using monoclonal antibody incubated with 6×His-tagged p29 recombinant protein shows no signal (*lane 2*). *B,* subcellular fractionation of cell extracts was prepared for Western blot analysis. *WCE,* whole cell extracts; *CE,* cytosolic extracts; *NE,* nuclear extracts; *P3,* chromatin-enriched fraction. β-Tubulin was used as a control. *C,* HeLa cells were preextracted by Triton X-100 alone or Triton X-100 plus DNase I and then fixed in cold methanol for immunofluorescence using anti-p29 monoclonal antibody. Anti-MCM3 polyclonal antibody was used as a positive control. DNA was stained with 4′,6-diamidino-2-phenylindole (*DAPI*). *D,* HeLa cells were arrested at G_1-S and released from the block. DNA content was measured by flow cytometry. Immunofluorescence staining was carried out in the G_1, S, G_2, and M phases using monoclonal anti-p29 antibody. Cyclin A was used as a marker to detect cells in S and G_2 phase. Astrin was a marker for M phase. *E,* HeLa cells released from thymidine/aphidicolin block were harvested at the indicated time points. The expression of cyclin A was shown as a control of cell cycle progression.

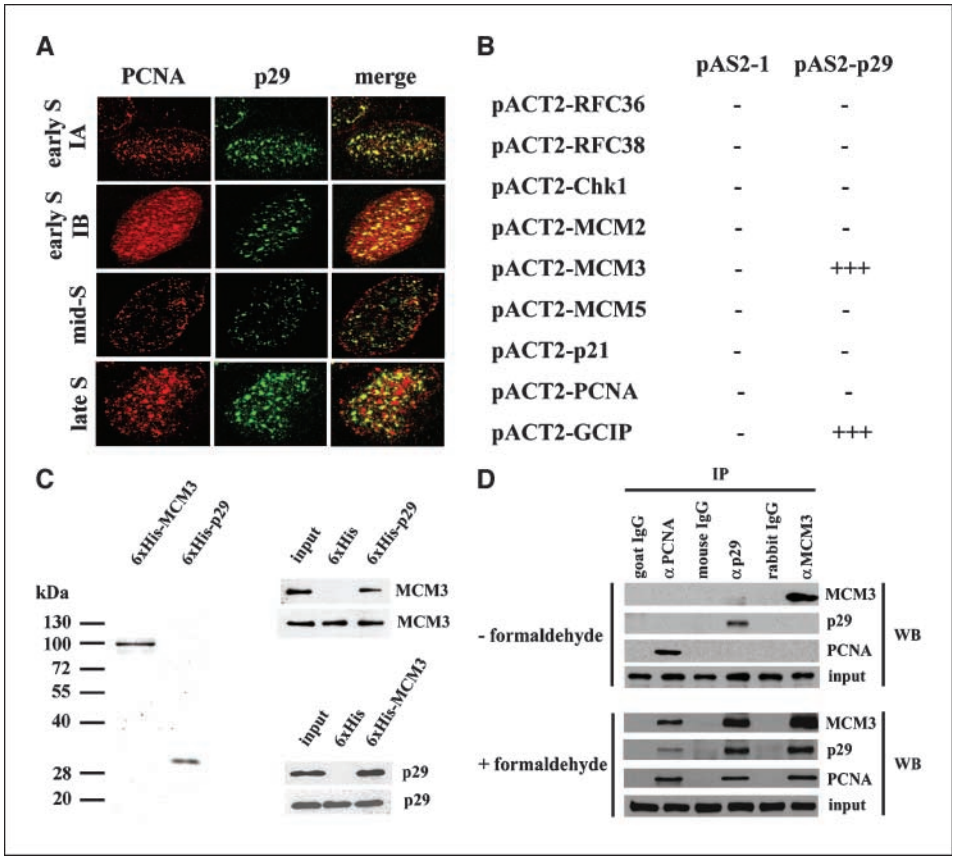

Figure 2. p29 localizes to replication foci and interacts with MCM3. *A,* HeLa cells were arrested at G_1-S with thymidine/aphidicolin and released with fresh medium. Cells were treated with 0.5% Triton X-100 and simultaneously labeled with a mixture of anti-p29 monoclonal antibody and anti-PCNA polyclonal antibody. The colocalized areas are overlaid by p29 and PCNA images (*yellow*). *B,* human RFC36, RFC38, Chk1, MCM2, MCM3, MCM5, p21, PCNA, and GCIP were constructed into pACT2 and cotransformed into yeast AH109 with pAS2-1 and pAS2-p29. +++, strong interaction according to *His3* expression and LacZ activity. *C,* 6×His-tagged p29 and MCM3 recombinant proteins were purified (*left*), immobilized onto Ni-NTA agarose, and incubated with HeLa cell extracts. Anti-p29 and anti-MCM3 antibodies were applied to detect an affinity complex. *D,* HeLa cells were arrested at G_1-S phase and released with fresh medium. Cells were either treated or untreated with formaldehyde and cell extracts were prepared and immunoprecipitated with p29, MCM3, and PCNA antibodies. Anti-goat, anti-mouse, and anti-rabbit IgGs were used as controls. *Input,* the same amount of cell extracts for immunoprecipitation blotted by anti-MCM2 antibody.

phase by a double thymidine/aphidicolin block and released from the block. Immunofluorescence showed that the majority of HeLa cells in G_1 phase had predominant nuclear staining, whereas cyclin A did not appear in the nucleus (Fig. 1*D*). Interestingly, as cyclin A entered the nucleus in early S phase, we found that p29 was stained in a pattern similar to replication foci. When cells progressed into the G_2 phase, there were again more nuclear signals similar to the G_1 phase. In the M phase, p29 mainly localized in the cytoplasm (Fig. 1*D*). Whole cell extracts and subcellular fractionation of p29 protein prepared at the indicated time points showed that p29 did not noticeably fluctuate with cell cycle progression (Fig. 1*E*), indicating that p29 protein might interact with other complexes to mask its antigenicity in the S phase.

MCM3 is a p29-interacting protein. To test if Triton-extraction resistant p29 foci correspond to sites of DNA replication, we coimmunostained Triton-extracted cells with p29 and proliferating cell nuclear antigen (PCNA). In the G_1 phase, p29 predominantly localized in the nucleus. By contrast, very little nuclear staining of PCNA was observed (data not shown). In the early S and late S stages, p29 and PCNA staining showed punctate areas of substantial, but not complete, overlap (Fig. 2*A*). It has been reported that PCNA foci appear at the nuclear periphery and scatter throughout the interior in the mid-S nuclei (23). Interestingly, p29 colocalized with PCNA in the interior of the nuclei, but not at the nuclear periphery, during the mid-S phase (Fig. 2*A*). PCNA-containing DNA replication foci contain many components involved in DNA synthesis, cell cycle progression, and checkpoint control (24). To isolate p29-interacting partners in the S phase, we constructed RFC36, RFC38, Chk1, MCM2, MCM3, MCM5, p21, and PCNA for the yeast-hybrid assay. GCIP was used as a positive control. We found that p29 interacted with MCM3 in the yeast-hybrid analysis (Fig. 2*B*). To investigate whether p29 interacts with MCM3 *in vitro*, cell lysates prepared from HeLa cells were incubated with either affinity-purified 6×His-p29 or 6×His-MCM3 recombinant proteins (Fig. 2*C, left*) and were analyzed by Western blotting. p29 and MCM3 were identified in the same affinity complex (Fig. 2*C, right*). Control experiments using empty vector did not show an association of p29 or MCM3 with Ni-NTA agarose, demonstrating that p29 could specifically interact with MCM3. To investigate whether p29 interacts with MCM3 in mammalian cells, HeLa cells were arrested by thymidine/aphidicolin block and chromatin immunoprecipitation was carried out. Due to the smaller amount of p29 present in the soluble nuclear extracts (Fig. 1*B*), we did not coimmunoprecipitate p29 and MCM3 from protein extracts without the treatment of formaldehyde (Fig. 2*D*). This may suggest a loose interaction between p29 and MCM3 in the absence of DNA. By contrast, chromatin-bound extracts immunoprecipitated with anti-p29, MCM3, or PCNA antibodies revealed that p29, MCM3, and PCNA were in the same immunocomplex. The control experiments using corresponding IgGs did not pull down p29, MCM3, or PCNA (Fig. 2*D*), indicating that these three proteins formed a tight complex in the presence of DNA during the S phase.

Silencing of p29 inhibits DNA replication. We employed two human p29 siRNA duplexes, sip29-1 and sip29-2, to knock down p29 expression. Firefly luciferase siRNA duplex was used as a control. The total amount of human p29 protein was significantly reduced at 48 and 72 hours after siRNA transfection and sip29-2 could more efficiently suppress the expression of p29 (Fig. 3*A*). We analyzed DNA synthesis using *in vivo* BrdUrd incorporation.

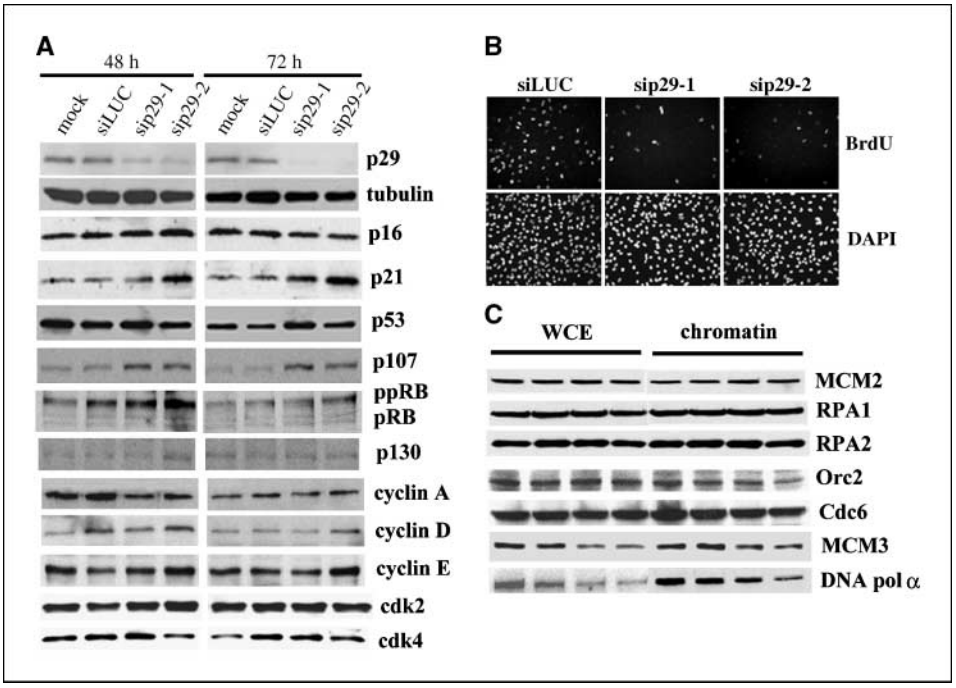

Figure 3. Silencing of p29 expression by siRNA. *A,* HeLa cells were transfected with control luciferase or p29 siRNA duplexes and cell extracts were prepared for Western blot analysis. β-Tubulin was used as a loading control. *B,* HeLa cells were transfected with siRNA duplexes for 72 hours, incubated with 50 μmol/L of BrdUrd for 30 minutes, and then chased with fresh medium for 1 hour. Immunofluorescence was carried out by anti-BrdUrd monoclonal antibody. *C,* whole cell extracts and chromatin-bound fraction were prepared to detect components of prereplication complex and replication complex.

A smaller amount of BrdUrd incorporation was observed in p29 siRNA–transfected cells (Fig. 3*B*), suggesting that DNA replication was impaired in p29-depleted cells. To decipher which component of G_1-S transition was affected in p29 knockdown cells, we examined the expression of cyclin A, cyclin D, cyclin E, cdk2, cdk4, and RB family. The depletion of p29 had no effect on the stability of these proteins and we did not detect significant changes of different RB species in p29-depleted cells (Fig. 3*A*). By contrast, p21 and p107 was elevated at 48 and 72 hours after siRNA transfection in HeLa cells (Fig. 3*A*). Cell extracts immunoprecipitated by anti-cyclin D or anti-cyclin E antibodies and *in vitro* H1 kinase assay did not show a significant reduction of phosphorylation on histone H1 (data not shown), indicating that the failure of S phase entry might not be through the inhibition of cyclin-cdk activity. Instead, we tested whether the ablation of p29 affected the assembly of prereplication complex onto chromatin. The associations of MCM2, RPA1, RPA2, Orc2, and cdc6 with chromatin were not remarkably decreased. In contrast, the total amount and the chromatin-associated fraction of MCM3 and DNA polymerase α were reduced, which in turn, could lead to an environment unfavorable for DNA replication (Fig. 3*C*).

Apoptosis in p29-depleted cells after UV irradiation. Furthermore, we checked whether p29-depleted cells were sensitive to genotoxic replication stress. A variety of UV dosages (10, 30, and 50 J/m^2) were employed to treat p29-depleted cells. Cell extracts were harvested at 1 hour after UV irradiation. Western blot analysis showed that the expression of Chk1 was suppressed and the phosphorylation of Chk1 at S317 and S345 could be reduced with a low dose (10 J/m^2) of UV irradiation (Fig. 4*A*). The expression of ATR, ATRIP, and Rad17 were unchanged in p29-depleted cells either with or without UV irradiation. We did not detect a significant mobility shift of ATRIP and a reduced phosphorylation of Rad17 at S645 (Fig. 4*A*), indicating that ATR activity might not be altered in p29-depleted cells. We found that 50 J/m^2 UV treatment rendered a maximum effect with flow cytometry analysis. To test whether the introduction of p29 siRNA affected cell cycle progression in response to UV irradiation, HeLa cells were transfected with siRNA duplexes for 72 hours, irradiated with UV light, and collected to measure DNA contents at the indicated time points post-UV irradiation. The majority of siRNA-transfected cells were in the G_1 phase before UV exposure. At 1 and 4 hours post-UV irradiation, most cells remained in the G_1 phase with minor shift of DNA contents (Fig. 4*B*). At 24 and 48 hours post-UV irradiation, the control luciferase siRNA-transfected cells increased in the G_2-M phase for DNA repair and ~40% of cells were in the G_1 phase. Nonetheless, more than 56% of p29-depleted HeLa cells accumulated in the G_1 phase (Fig. 4*B*). A significant increase in the sub-G_1 population was observed in p29-2 siRNA-transfected cells at 48 hours post-UV irradiation (Fig. 4*B*). Similarly, an increment in the apoptotic population of p29-depleted cells with Annexin V staining was found after UV irradiation (Fig. 4*B, right*), indicating that the silencing of p29 not only impaired DNA synthesis but also resulted in apoptosis. The polyclonal anti-pChk1 S345 antibody was not applicable in immunofluorescence. Nonetheless, immunofluorescent detection of pChk1 at S317 showed a significant decrease in p29 siRNA-transfected cells (Fig. 4*C*), supporting the contention that Chk1 activity was inhibited by UV irradiation. Premature chromosome condensation is a lethal event in mammalian cells entering mitosis with uncompleted replicated DNA. This event is preventable by ATR kinase via Chk1 activation (21, 22). Because the phosphorylation levels of Chk1 at S317 and S345 were suppressed, we checked whether the depletion of p29 resulted in premature chromosome condensation with UV irradiation. At least 300 mitotic spreads were counted in each experiment. Approximately 13% of luciferase siRNA-transfected cells showed typical apoptotic bodies with very little premature chromosome condensation. By contrast, 29% of p29 siRNA-transfected cells showed apoptotic bodies and 8% of p29-depleted cells displayed widespread fragmentation of chromosomes with representative characteristics of premature chromosome condensation (Fig. 4*C*), indicating that p29-depleted cells with incompletely replicated DNA did not have

sufficient Chk1 activity to delay cell entry to mitosis, resulting in premature chromosome condensation and cell death.

To clarify whether the phenotype of p29 knockdown is specific to HeLa cells, HCT116 colon cancer cells containing an intact p53 tumor suppressor protein were transfected with siRNA duplexes and subjected to similar analyses. Immunoblotting showed that p107 was elevated. The phosphorylation levels of Chk1 at S317/S345 and RPA2 were decreased (Fig. 4*D*), ruling out the possibility that p29 siRNA-induced UV sensitization occurs only in HeLa cells.

Silencing of p29 inhibits ATM phosphorylation after UV irradiation. To test whether the depletion of p29 regulates ATM activity, HeLa cells were transfected with siRNA duplexes for 72 hours and then exposed with 50 J/m^2 UV light. A time course study was conducted. The phosphorylation of ATM at S1981 was elevated in mock and luciferase siRNA-transfected cells at 1 hour after UV irradiation. Nonetheless, the phosphorylation of ATM at S1981 in p29-depleted cells was significantly reduced (Fig. 5*A*), whereas siRNA-transfected cells showed little change in DNA content at this time point (Fig. 4*B*), indicating that the defective ATM phosphorylation is an early event but not a delayed cell cycle effect in p29-silenced cells in response to UV treatment. Because the activation and phosphorylation of ATM at S1981 is highly dependent on MRN complex in double-strand breaks, we measured the expression of Mre11, Rad50, and Nbs1. The total amounts of ATM, Mre11, Nbs1, and Rad50 were unchanged (Fig. 5*A*), indicating that the inhibited phosphorylation of ATM at S1981 was not due to the down-regulated expression of ATM or MRN complex. The phosphorylation of ATM downstream targets, Chk2 at T68 and RPA2, was also reduced (Fig. 5*A*). The phosphorylation of RPA2, one of the ATM substrates (25, 26), was reduced after 4 hours with a delayed effect, supporting that the ATM kinase activity was suppressed in p29-depleted cells. Furthermore, we tested whether the reduced phosphorylation of ATM at S1981 also occurred with the treatment of hydroxyurea or ionizing irradiation. Intriguingly, the phosphorylation of ATM at S1981 was not inhibited in response to hydroxyurea and ionizing irradiation in p29-depleted cells (data not shown), suggesting that p29 only affects the phosphorylation of ATM after UV irradiation. We checked whether p29 specifically colocalized with ATM S1981 in UV but not in hydroxyurea or ionizing irradiation treatment. As expected, p29 colocalized with ATM S1981 in distinct foci in UV-irradiated cells. In contrast, p29 did not colocalize with ATM S1981 in hydroxyurea- or ionizing irradiation–treated cells (Fig. 5*B*), suggesting that p29 is required for the activation and phosphorylation of ATM in response to UV irradiation.

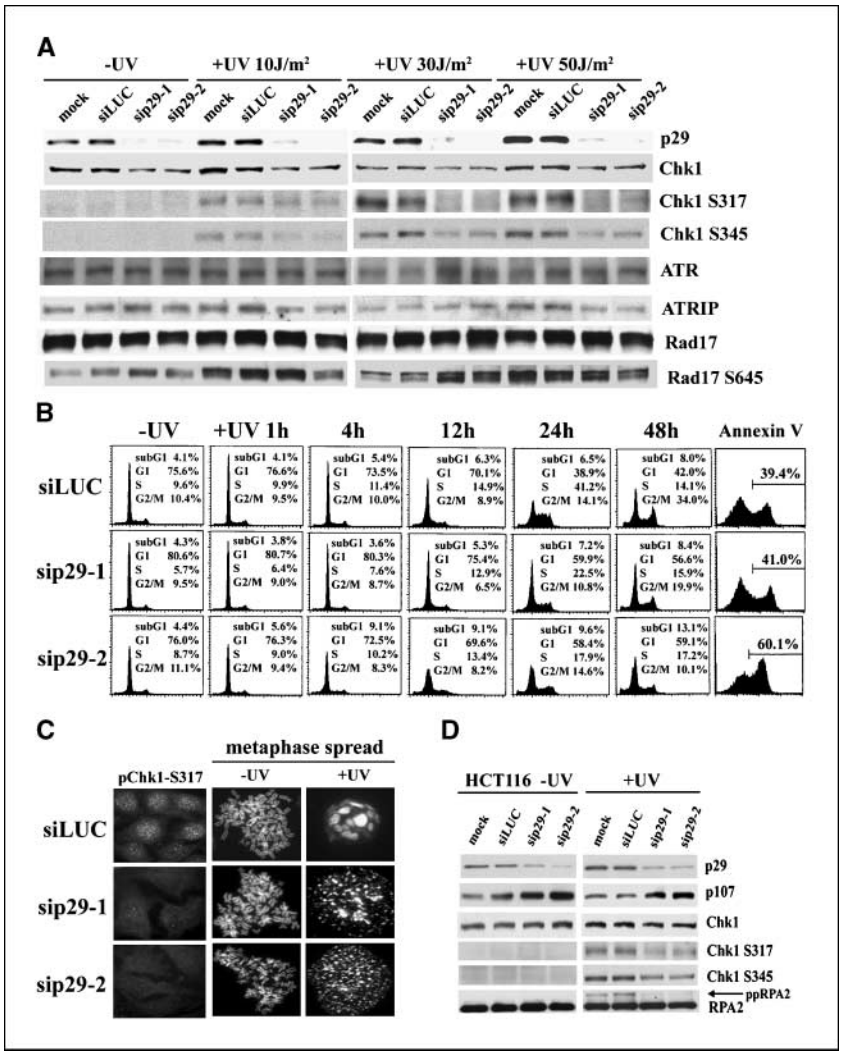

Figure 4. Apoptosis and suppressed Chk1 phosphorylation in p29-depleted cells after UV irradiation. HeLa cells were transfected with siRNA duplexes for 72 hours and then irradiated with different dosages of UV light. Cell extracts were harvested at 1 hour post-UV treatment. *A,* Western blot was carried out using anti-Chk1, Chk1 S317, Chk1 S345, ATR, ATRIP, Rad17, and Rad17 S645 antibodies. *B,* DNA content was determined by flow cytometry at the indicated time points post-UV exposure (50 J/m^2). Apoptotic cells were labeled with FITC-conjugated Annexin V and propidium iodide for flow cytometry analysis at 48 hours post-UV irradiation (*right*). *C,* cells were fixed and immunofluorescence was done using anti-Chk1 S317 antibody (*left*). Mitotic chromosome spreads were prepared with or without UV treatment as described in Materials and Methods. *D,* colon cancer HCT116 cells were transfected with siRNA duplexes and subjected to UV irradiation. Immunoblotting was conducted with the indicated antibodies.

Discussion

On the basis of these experiments, we conclude that the depletion of p29 has three effects on cell cycle progression and DNA damage checkpoint responses. First, the knockdown of p29 induces higher expression of p21 and p107 and down-regulated expression of DNA polymerase α, which could arrest cells in the G_1 phase and negatively regulate the process of DNA synthesis. Second, p29 deficiency resulted in a decreased Chk1 activity and premature chromatin condensation after UV irradiation. Third, p29 is required for UV-induced ATM phosphorylation at S1981 in HeLa cells (Fig. 6).

The licensing of DNA replication origin requires CDC6 and CDT1, which interact with the origin-of-replication complex to load MCM2-7 onto chromatin. Subsequently, DNA replication proteins, such as PCNA, RPA, RFC, DNA polymerase α and ε, triggers the initiation of DNA replication (27–30). MCM2-7 proteins are mini-chromosome maintenance proteins that display ATPase activity and all six are required both for the initiation and elongation of DNA replication. The MCM2-7 complex loaded onto replication origins takes place during late mitosis and the G_1 phase for the next round of chromosome replication (27–30). Additionally, MCM4 is phosphorylated by ATR-Chk1 and Cdk2 kinases, which inhibits DNA replication and blocks DNA fork progression (31). MCM3 is phosphorylated in cells exposed to ionizing irradiation, UV, and hydroxyurea. ATM is responsible for the phosphorylation of MCM3 on S535 and ATR phosphorylates MCM2 on S108 in response to multiple forms of DNA damage and stalling of replication forks (32). It remains unclear whether p29 is directly involved in the formation of the pre–origin-of-replication complex. Because the total amount of MCM3 was decreased in p29-depleted cells (Fig. 3*C*), it would be plausible to predict that the phosphorylation of MCM3 was decreased in p29-depleted cells irradiated with UV light. Thus, the down-regulated and hypo-phosphorylated MCM3 may impair DNA replication in response to UV irradiation.

Chromatin immunoprecipitation and genomewide analysis of promoters occupied by E2F transcription factors has identified many genes responsible for cell cycle progression, DNA replication, and DNA damage/repair checkpoints (33–36). Among these E2F-regulated genes, p21 inhibits Cdk activity and interacts with PCNA to suppress DNA replication (37, 38). p107 mainly interacts with E2F4 and E2F5, and overexpression of p107 can inhibit G_1 to S phase progression by down-regulating the expression of the F-box protein Skp2 (39). It would not be surprising to find that DNA replication in p29 knockdown cells was inhibited because the expression of p21 and p107 were increased. Nevertheless, candidate genes that can be regulated by the E2F family, like cyclin A, MCM2, CDC6, and Orc2, were not affected in p29-depleted cells, indicating that the activity of E2F transcription factors selectively activates or represses the expression levels of some targeted genes

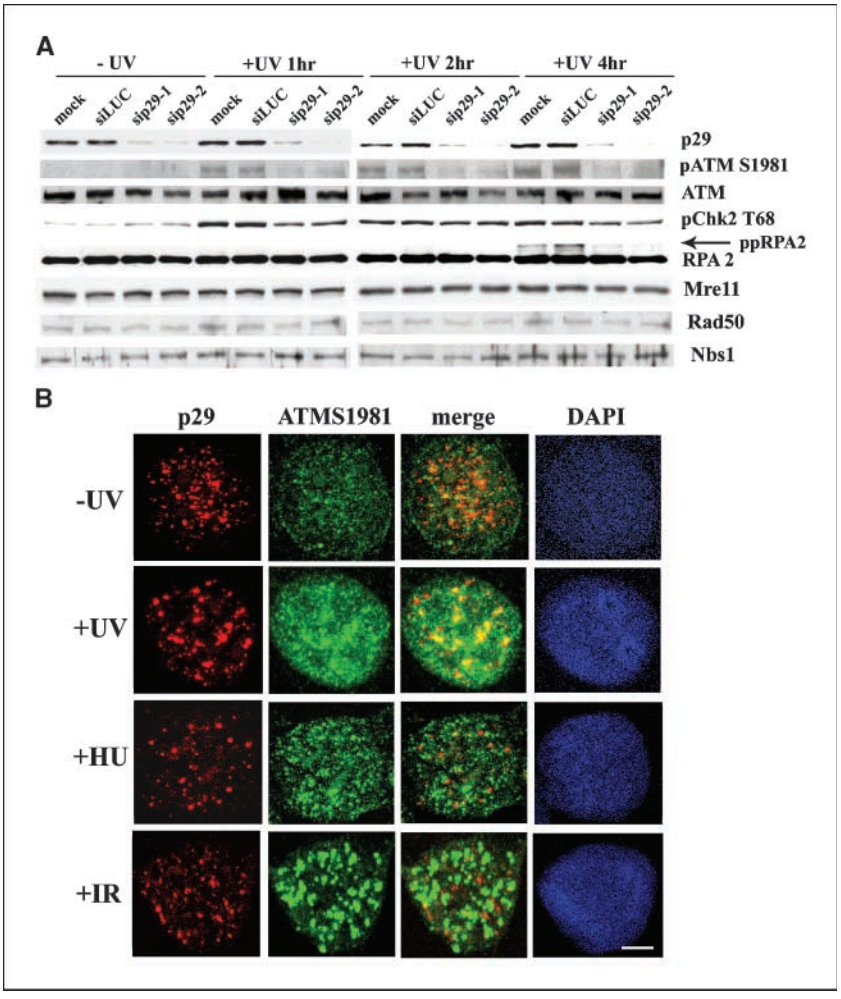

Figure 5. Inhibition of ATM phosphorylation in p29-depleted cells after UV irradiation. *A,* HeLa cells were transfected with control or p29 siRNA duplexes for 72 hours and then UV irradiated (50 J/m^2). Cell extracts were collected at the indicated time points and Western blotting was carried out using anti-ATM S1981, ATM, pChk2 T68, RPA2, Mre11, Rad50, and Nbs1 antibodies. *B,* cells transfected with siRNA duplexes were treated with UV (50 J/m^2), hydroxyurea (1 mg/mL), or ionization irradiation (10 Gy), extracted with Triton X-100, and fixed with cold methanol. Immunofluorescence staining was simultaneously done using anti-p29 and anti-ATM S1981 antibodies. *Bar,* 10 μm.

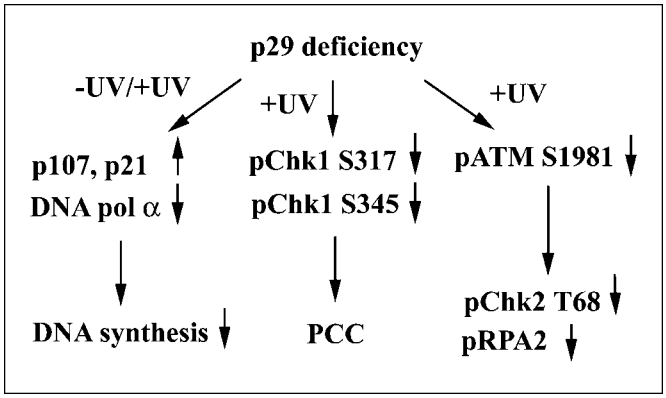

Figure 6. A schematic model for silencing of p29 in the DNA damage checkpoint pathway. Without UV irradiation, the p29 depletion induces p107 and p21 and down-regulates DNA polymerase α, which could lead to an inhibition of DNA synthesis. The low phosphorylation of Chk1 at S317 and S345 could result in premature chromatin condensation (*PCC*) with UV treatment. The phosphorylation of ATM at S1981 is inhibited in response to UV irradiation. Consequently, the phosphorylation levels of Chk2 and RPA2, downstream targets of ATM, are also suppressed.

in p29-depleted cells. Another possibility is that p29 acts as a transcriptional activator or repressor in collaboration with E2F to control the expression of some E2F-regulated genes, thereby regulating the protein levels of specific genes in cell cycle progression.

Previous studies have shown that the ablation of Chk1 by siRNA has only a small effect on the accumulation of sub-G_1 cells or other phases of the cell cycle (40), indicating that the decreased expression of Chk1 may not be responsible for the G_1 arrest in p29-depleted cells. In contrast, Chk1 is mainly recognized as a signal-transducing kinase in the DNA damage checkpoint pathway, like UV light or stalled replication stress (41–45). The phosphorylation of Chk1 at Ser^{317} and Ser^{345} is highly associated with its ability to phosphorylate downstream targets, like cdc25A, cdc25C, and p53 (41–45). The depletion of p29 did not affect the expression of ATR and ATM (Figs. 4*A* and 5*A*). Therefore, the low phosphorylation level of Chk1 at S317 and S345 might be mainly due to down-regulated expression of Chk1. Subsequently, the decreased Chk1 activity did not provide enough checkpoint activity in response to genotoxic stress. We did not detect any interaction between p29 and Chk1 using the yeast two-hybrid assay (Fig. 2*A*), indicating that p29 may not be responsible for the stability of Chk1 through direct interaction. Instead, this down-regulated expression of Chk1 is most likely related to transcriptional repression of induced E2F4 protein, as has been suggested in a previous microarray analysis (34).

Another important observation in this study was that p29 was required for maximal phosphorylation of ATM kinase in UV-induced responses. In p29-depleted cells, the phosphorylation of ATM was inhibited but the total amount of ATM was not altered. The hypophosphorylated ATM may have further resulted in decreased phosphorylation of Chk2 and RPA2 in response to UV irradiation (Fig. 5*A*). Like other DNA repair and checkpoint proteins, the expression of ATM, Chk2, and RPA2 can be modulated by the E2F family (46, 47). In our observations, no significant reduction of ATM, Chk2, and RPA2 in p29-depleted cells was detected (Fig. 5*A*), suggesting that E2F and p107 did not affect the expression of these three protein in p29-depleted cells. Although it is believed that the MRN formed at double-strand breaks is necessary for ATM activity (11–13), the mechanism for ATM activation with UV treatment is unclear. The expression of Mre11, Nbs1, and Rad50 remained stable in p29-depleted cells. Thus, it is unlikely that the decreased ATM phosphorylation is mediated by a down-regulated expression of MRN complex. Intriguingly, this down-regulated phosphorylation of ATM did not occur in p29-depleted cells exposed to hydroxyurea or ionization radiation. One possibility is that UV irradiation induces a local chromatin modification to activate ATM phosphorylation and p29 is required for this unique modulation of ATM activity. Although we provide the evidence that p29 colocalizes with ATM after UV irradiation, a mechanism for p29 to affect ATM phosphorylation is far from certain. Nonetheless, our data do help to partially unravel the role of p29 in cell cycle control and DNA checkpoint responses.

Acknowledgments

Received 9/12/2005; revised 5/22/2006; accepted 6/27/2006.

Grant support: National Science Council to Y.C. Yang (NSC 94-2314-B-195-021) and M.S. Chang (NSC 94-2311-B-195-002).

The costs of publication of this article were defrayed in part by the payment of page charges. This article must therefore be hereby marked *advertisement* in accordance with 18 U.S.C. Section 1734 solely to indicate this fact.

We are grateful to Drs. Tso-Pang Yao and Mei-Ling Kuo for critical comments and Dr. Mary Jeanne Buttrey for helpful reading on this article.

References

1. Massagué J. G1 cell cycle control and cancer. Nature 2004;432:298–306.
2. Murray AW. Recycling the cell cycle: cyclins revisited. Cell 2004;116:221–34.
3. Sherr CJ, Roberts JM. Living with or without cyclins and cyclin-dependent kinases. Genes Dev 2004;18:2699–711.
4. Stevaux O, Dyson NJ. A revised picture of the E2F transcriptional network and RB function. Curr Opin Cell Biol 2002;14:684–91.
5. Cam H, Dynlacht BD. Emerging roles for E2F: beyond the G1/S transition and DNA replication. Cancer Cell 2003;3:311–6.
6. Cobrinik D. Pocket proteins and cell cycle control. Oncogene 2005;24:2796–809.
7. Kastan MB, Bartek J. Cell-cycle checkpoints and cancer. Nature 2004;432:316–23.
8. Lukas J, Lukas C, Bartek J. Mammalian cell cycle checkpoints: signalling pathways and their organization in space and time. DNA Repair 2004;3:997–1007.
9. Sancar A, Lindsey-Boltz LA, Ünsal-Kaçmaz K, Linn S. Molecular mechanisms of mammalian DNA repair and the DNA damage checkpoints. Annu Rev Biochem 2004; 73:39–85.
10. McKinnon PJ. ATM and ataxia telangiectasia. EMBO Rep 2004;5:772–6.
11. Uziel T, Lerenthal Y, Moyal L, Andegeko Y, Mittelman L, Shiloh Y. Requirement of the MRN complex for ATM activation by DNA damage. EMBO J 2003;22:5612–21.
12. Lee JH, Paull TT. Direct activation of the ATM protein kinase by the Mre11/Rad50/Nbs1 complex. Science 2004;304:93–6.
13. Lee JH, Paull TT. ATM activation by DNA double-strand breaks through the Mre11/Rad50/Nbs1 complex. Science 2005;308:551–4.
14. Bartek J, Lukas C, Lukas J. Checking on DNA damage in S phase. Nat Rev Mol Cell Biol 2004;5:792–804.
15. Osborn AJ, Elledge SJ, Zou L. Checking on the fork: the DNA-replication stress-response pathway. Trends Cell Biol 2002;12:509–16.
16. Parrilla-Castellar ER, Arlander SJ, Karnitz L. Dial 9-1-1 for DNA damage: the Rad9-1-Rad1 (9-1-1) clamp complex. DNA Repair 2004;3:1009–14.
17. Chang MS, Chang CL, Huang CJ, Yang YC. p29, a novel GCIP interacting protein, localizes in the nucleus. Biochem Biophys Res Commun 2000;279: 732–7.
18. Xia C, Bao Z, Tabassam F, et al. GCIP, a novel human Grap2 and cyclin D interacting protein, regulates E2F-mediated transcriptional activity. J Biol Chem 2000;275: 20942–8.
19. Méndez J, Stillman B. Chromatin association of human origin recognition complex, cdc6, and mini-chromosome maintenance proteins during the cell cycle: assembly of prereplication complexes in late mitosis. Mol Cell Biol 2000;20:8602–12.
20. Kang SHL, Vieira K, Bungert J. Combining chromatin immunoprecipitation and DNA footprinting: a novel method to analyze protein-DNA interactions *in vivo*. Nucleic Acids Res 2002;30:e44–8.
21. Nghiem P, Park PK, Kim Y, Vaziri C, Schreiber SL. ATR inhibition selectively sensitizes G1 checkpoint-deficient

cells to lethal premature chromatin condensation. Proc Natl Acad Sci U S A 2001;98:9092–7.
22. Nghiem P, Park PK, Kim Y, Desai BN, Schreiber SL. ATR is not required for p53 activation but synergizes with p53 in the replication checkpoint. J Biol Chem 2002;277:4428–34.
23. Dimitrova DS, Berezney R. The spatio-temporal organization of DNA replication sites is identical in primary, immortalized and transformed mammalian cells. J Cell Sci 2002;115:4037–51.
24. Maga G, Hübscher U. Proliferating cell nuclear antigen (PCNA): a dancer with many partners. J Cell Sci 2003;116:3051–60.
25. Matsuoka S, Rotman G, Ogawa A, Shiloh Y, Tamai K, Elledge SJ. Ataxia telangiectasia-mutated phosphorylates Chk2 *in vivo* and *in vitro*. Proc Natl Acad Sci U S A 2000;97:10389–94.
26. Oakley GG, Loberg LI, Yao J, et al. UV-induced hyperphosphorylation of replication protein A depends on DNA replication and expression of ATM protein. Mol Biol Cell 2001;12:1199–213.
27. Bell SP, Dutta A. DNA replication in eukaryotic cells. Annu Rev Biochem 2002;71:333–74.
28. Mendez J, Stillman B. Perpetuating the double helix: molecular machines at eukaryotic DNA replication origins. Bioessays 2003;25:1158–67.
29. Hyrien O, Marheineke K, Goldar A. Paradoxes of eukaryotic DNA replication: MCM proteins and the random completion problem. Bioessays 2003;25:116–25.
30. Bailis JM, Forsburg SL. MCM proteins: DNA damage, mutagenesis and repair. Curr Opin Genet Dev 2004;14:17–21.
31. Ishimi Y, Komamura-Kohno Y, Kwon HJ, Yamada K, Nakanishi M. Identification of MCM4 as a target of the DNA replication block checkpoint system. J Biol Chem 2003;278:24644–50.
32. Cortez D, Glick G, Elledge SJ. Minichromosome maintenance proteins are direct targets of the ATM and ATR checkpoint kinases. Proc Natl Acad Sci U S A 2004;101:10078–83.
33. Takahashi Y, Rayman JB, Dynlacht BD. Analysis of promoter binding by the E2F and pRB families *in vivo*: distinct E2F proteins mediate activation and repression. Genes Dev 2000;14:804–16.
34. Ishida S, Huang E, Zuzan H, et al. Role for E2F in control of both DNA replication and mitotic functions as revealed from DNA microarray analysis. Mol Cell Biol 2001;21:4684–99.
35. Ren B, Cam H, Takashashi Y, et al. E2F integrates cell cycle progression with DNA repair, replication, and G2/M checkpoints. Genes Dev 2002;16:245–56.
36. Cam H, Balciunaite E, Blais A, et al. A common set of gene regulatory networks links metabolism and growth inhibition. Mol Cell 2004;16:399–411.
37. Waga S, Hannon GJ, Beach D, Stillman B. The p21 inhibitor of cyclin-dependent kinases controls DNA replication by interaction with PCNA. Nature 1994;369:574–8.
38. Luo Y, Hurwitz J, Massagué J. Cell-cycle inhibition by independent CDK and PCNA binding domains in $p21^{Cip1}$. Nature 1995;375:159–61.
39. Rodier G, Makris C, Coulombe P, et al. p107 inhibits G1 to S phase progression by down-regulating expression of the F-box protein Skp2. J Cell Biol 2005;168:55–66.
40. Rodriguez R, Meuth M. Chk1 and p21 cooperate to prevent apoptosis during DNA replication fork stress. Mol Biol Cell 2006;17:402–12.
41. Bartek J, Lukas J. Chk1 and Chk2 kinases in checkpoint control and cancer. Cancer Cell 2003;3:421–9.
42. Chen Y, Sanchez Y. Chk1 in the DNA damage response: conserved roles from yeasts to mammals. DNA Repair 2004;3:1025–32.
43. Zhao H, Piwnica-Worms H. ATR-mediated checkpoint pathways regulate phosphorylation and activation of human Chk1. Mol Cell Biol 2001;21:4129–39.
44. Jiang K, Pereira E, Maxfield M, Russell B, Goudelock DM, Sanchez Y. Regulation of Chk1 includes chromatin association and 14-3-3 binding following phosphorylation on Ser-345. J Biol Chem 2003;278:25207–17.
45. Helt CE, Cliby WA, Keng PC, Bambara RA, O'Reilly MA. Ataxia telangiectasia-mutated (ATM) and ATM and Rad3-related protein exhibit selective target specificities in response to different forms of DNA damage. J Biol Chem 2005;280:1186–92.
46. Berkovich E, Ginsberg D. ATM is a target for positive regulation by E2F-1. Oncogene 2003;22:161–7.
47. Kalma Y, Marash L, Lamed Y, Ginsberg D. Expression analysis using DNA microarrays demonstrates that E2F-1 up-regulates expression of DNA replication genes including replication protein A2. Oncogene 2001;20:1379–87.